Available online at www.sciencedirect.com
SCIENCE DIRECT®
International Journal of Thermal Sciences 42 (2003) 85–94
International Journal of Thermal Sciences
www.elsevier.com/locate/ijts

Absorption of organic fluid mixtures in plate heat exchangers

Manel Vallès, Mahmoud Bourouis, Dieter Boer, Alberto Coronas *

Center of Technological Innovation in Energy Upgrading and Refrigeration (CREVER), Universitat Rovira i Virgili, Autovia de Salou, 43006 Tarragona, Spain

Received 3 September 2001; accepted 6 March 2002

Abstract

It is well known that the absorber is the key component in energy conversion systems that are based on absorption cycles. This paper describes an experimental investigation into the absorption process of organic fluid mixtures in an absorption system which has a spray and a plate heat exchanger. The absorber consists of an adiabatic mixing chamber with a spray, where the solution that is weak in refrigerant is sprayed into the refrigerant vapour. A two-phase mixture is formed and enters a plate heat exchanger, where the solution is cooled to complete the absorption process.

We carried out experiments with different types of spray nozzles using the organic fluid mixtures methanol–tetraethyleneglycol dimethylether (TEGDME) and trifluoroethanol (TFE)–TEGDME. We analyse how the solution mass flow rate, absorber pressure and cooling water temperature affected the absorber performance and we discuss the results in terms of the absorber load, absorbed mass flux, degree of subcooling of the solution at the absorber outlet, solution film heat and mass transfer coefficients.

The results indicate that the absorption system proposed is suitable for relatively low pressures. For water temperatures of 30 °C and absorber pressures between 2 and 6 kPa, the absorption rates for TFE–TEGDME were 1 to 2.5 $g{\cdot}s^{-1}{\cdot}m^{-2}$. The corresponding values for methanol–TEGDME with absorber pressures between 10 and 15 kPa were 0.4 to 1.2 $g{\cdot}s^{-1}{\cdot}m^{-2}$.

Keywords: Absorber; Organic fluid mixtures; Methanol; Trifluoroethanol; Tetratehyleneglycol dimethylether; Plate heat exchangers; Spray

1. Introduction

Nowadays energy conversion systems based on absorption cycles use two inorganic fluid mixtures. The water–LiBr mixture is principally used for air-conditioning, chillers and heat transformers, and the ammonia–water mixture for refrigeration systems. These classical mixtures have some drawbacks. The operating range for water–LiBr is limited by the freezing point of water and crystallisation. The ammonia–water mixture needs rectification and is not suitable for double-effect cycles because of the high operation pressures required. Some of these problems can be avoided if such organic fluid mixtures as TFE–TEGDME [1–6] and methanol–TEGDME are used [7–10]. These organic fluid mixtures are suitable for double effect cycles, and the refrigerant can evaporate below 0 °C. Thus, efficiencies can be high and the fluid mixtures can be used in both cooling and heating modes. Moreover, these organic fluid mixtures have no crystallisation problems, which means that the range of the operating conditions can be extended. The temperature lift between the evaporator and the absorber can be about 50 K, so a dry cooling tower may be used to cool the absorber and condenser instead of a wet tower.

The drawbacks of organic fluids are that their transport properties are poor, which hampers the absorption process. Organic fluid mixtures have been tested basically in heat transformers [11] where the operating conditions make the use of inorganic fluid mixtures unsuitable.

The operating conditions of the absorbers in air conditioning or refrigerating machines are very different from those of heat transformers since temperatures and pressures are low and viscosities are high.

Although there is very little published data on absorption for the organic fluid mixtures, Ishikawa et al. [6] show that the absorption in falling film on horizontal tubes with TFE–TEGDME is lower than that with water–LiBr. They also reported the heat and mass transfer processes are improved if TFE–DMI is used in combination with advanced surface type laminated plates CCS (Constant Curvature Surface).

* Correspondence and reprints.
E-mail address: crever@crever.urv.es (A. Coronas).

1290-0729/02/$ – see front matter
PII: S1290-0729(02)00011-X

Nomenclature

A	surface area of the plate heat exchanger	m^2
b	channel pitch	m
cp	specific heat	$kJ{\cdot}kg^{-1}{\cdot}K^{-1}$
h	specific enthalpy	$kJ{\cdot}kg^{-1}$
j	absorption rate	$kg{\cdot}s^{-1}{\cdot}m^{-2}$
K	overall mass transfer coefficient	$m{\cdot}s^{-1}$
k	conductivity	$W{\cdot}m^{-1}{\cdot}K^{-1}$
m	mass flow rate	$kg{\cdot}s^{-1}$
P	pressure	kPa
Pr	Prandlt number, $= cp \cdot \mu \cdot k^{-1}$	
Q	heat transfer rate	kW
Re	Reynolds number, $= V \cdot 2b \cdot \nu^{-1}$	
T	temperature	°C
U	overall heat transfer coefficient	$W{\cdot}m^{-2}{\cdot}K^{-1}$
V	velocity	$m{\cdot}s^{-1}$
x	concentration of refrigerant in solution	% by weight

Greek symbols

α	film heat transfer coefficient	$W{\cdot}m^{-2}{\cdot}K^{-1}$
ΔT_{LM}	logarithmic-mean temperature difference	K
ΔC_{LM}	logarithmic-mean concentration difference	$kg{\cdot}m^{-3}$
δ	plate thickness	m
μ	dynamic viscosity	$kg{\cdot}m^{-1}{\cdot}s^{-1}$
ρ	density	$kg{\cdot}m^{-3}$
ν	kinematic viscosity	$m^{-2}{\cdot}s^{-1}$

Subscripts

a	absorber
cw	cooling water
eq	equilibrium
i	inlet
o	outlet
ref	refrigerant
s	strong solution leaving the plate heat exchanger
v	vapour
w	weak solution entering the mixing chamber

These considerations led us to select an absorption system for the above-mentioned organic fluid mixtures composed of a standard plate heat exchanger. We tested several different spray nozzles to distribute the solution into the channels of the plate heat exchanger. We analysed the performance of the system for each spray nozzle type under different operation parameters.

2. Description of the absorption system

The absorber was integrated into a double effect absorption–compression heat pump, in which a compressor is placed between the evaporator and the absorber to boost the absorber pressure. The cycle configuration has been described by Boer et al. [12].

In order to combine the advantages of both falling film and spray, the absorber has two parts (Fig. 1(a)). The absorption process takes place first in an adiabatic mixing chamber (Fig. 1(b)), where the weak solution is sprayed into the refrigerant vapour. Then, the two-phase mixture enters a plate heat exchanger, where the solution is cooled and the absorption process is completed. Finally, the solution that is strong in refrigerant is stored in the tank before it is pumped to the generator.

2.1. Spray nozzle type

Our choice of spray nozzle[1] took into account the geometry of a plate heat exchanger with a port diameter of 50 mm. Therefore, we chose spray nozzles with a small angle of aspersion. We also only selected sprays with a mean drop diameter greater than 0.2 mm, to limit the capillary pressure. These restrictions led to the sprays listed in Table 1. The values given in the table were facilitated by the manufacturer for water at 21 °C.

2.2. Plate heat exchanger

The plate heat exchanger (model CB76L)[2] is a standard welded exchanger and consists of 60 type L plates, particularly suitable for low-pressure drop applications and with a total surface area of 5.5 m^2. Table 2 shows the plate heat exchanger specifications.

2.3. Instrumentation

The parameters measured were:

- Temperature of the vapour at the compressor outlet;
- Temperature of the weak solution before spraying;
- Temperature of the strong solution at the outlet of the absorber;
- Inlet and outlet cooling water temperatures;
- Density, temperature and mass flow rate of the strong and weak solutions;
- Volume flow rate of the cooling water;
- Absolute pressures at the entrance of the absorber and in the solution tank.

[1] Manufactured by Spraying Systems Co.

[2] Manufactured by Alfa Laval.

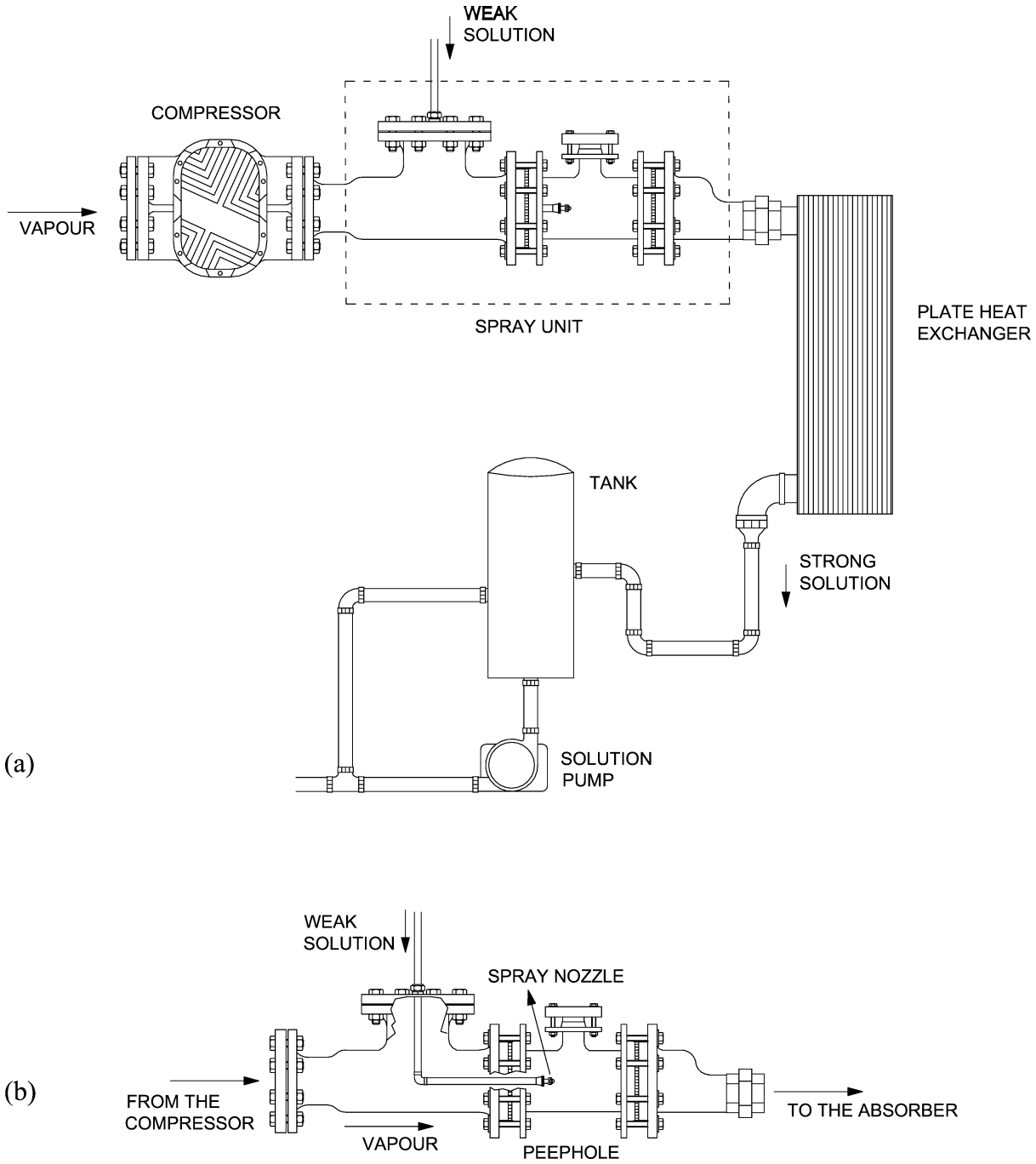

Fig. 1. Schematic diagram of the absorber unit: (a) absorber unit; (b) detail of adiabatic absorption chamber.

Table 3 shows the instrumentation and the accuracy of the measurements. The absorber pressure is set to the desired value by varying the compressor speed. In the experiments, the solution mass flow rate ranged between 200 and 400 $kg{\cdot}h^{-1}$ and the cooling water temperature between 30 and 40 °C at a mass flow rate of 3000 $kg{\cdot}h^{-1}$. In these conditions, the cooling water side heat transfer coefficient is about 1750 $W{\cdot}m^{-2}{\cdot}K^{-1}$; thus the dominant resistance to heat transfer is located on the solution side. The temperature of the weak solution entering the absorber was kept 5 K above that of the strong solution leaving the absorber.

The parameters measured were collected by a data acquisition system. The variables cooling water inlet temperature, strong solution mass flow rate and inlet absorber pressure were monitored with PID controllers.

2.4. Data validation

The operation data are affected by random and systematic errors, caused by perturbations in the process, deviations from steady state, problems with instrumentation, etc. As a consequence, there are some discrepancies in the mass and

Table 1
Characteristics of the spray nozzles

Spray nozzle	Spray type	Spray shape	Degree of aspersion	Capacity ($l \cdot min^{-1}$)	Mean droplet diameter (μm)
3/8 HHSJ-6007	Spiral	Full cone	60° (at 0.7 bar)	5.5 (at 3.0 bar)	200 (at 2.5 bar)
1/4 BSJ-5007	Spiral	Hollow cone	50° (at 0.7 bar)	5.5 (at 3.0 bar)	170 (at 2.5 bar)
3/8 B-5	Whirljet	Hollow cone	73° (at 1.4 bar)	3.2 (at 2.74 bar)	420 (at 2.74 bar)
1/4 G-3030 HC	Hollowjet	Hollow cone	28° (at 0.7 bar)	3.0 (at 2.74 bar)	1100 (at 2.74 bar)
1/4 G-6.50	Fulljet	Full cone	50° (at 1.4 bar)	4.3 (at 2.74 bar)	1780 (at 2.74 bar)
1/8 G-1514	Fulljet	Full cone	15° (at 2.74 bar)	5.3 (at 2.74 bar)	1115 (at 3 bar)
3/8 G-3014	Fulljet	Full cone	30° (at 2.74 bar)	5.3 (at 2.74 bar)	1780 (at 2.74 bar)

energy balances. Filtering the measurements using the data validation should reduce these problems. This methodology consists of two steps: systematic errors detection and data reconciliation. The data reconciliation problem is formulated as a constrained least squares estimation problem, in which the weighted least square differences between the measured and reconciled values are minimised subject to mass and energy balance restrictions.

The balances used are:

Global mass balance

$$m_s - m_{\text{ref}} - m_w = 0 \tag{1}$$

Refrigerant mass balance

$$m_s x_s - m_w x_w - m_{\text{ref}} = 0 \tag{2}$$

Energy balance

$$m_{\text{cw}} cp_{\text{cw}}(T_{\text{cw},o} - T_{\text{cw},i}) + m_s h_s[T_s, x_s] - m_{\text{ref}} h_{\text{ref}}\lfloor T_{\text{ref}}, P_a \rfloor - m_w h_w[T_w, x_w] = 0 \tag{3}$$

Table 2
Characteristics of the plate heat exchanger type CB76L used as absorber

Manufacturer	Alfa-laval
Unit type	CB76L
Number of plates	60
Plate pattern	L
Channel pitch (mm)	2.5
Plate thickness (mm)	0.4
Plate material	AISI 316
Channel volume (l)	0.26
Width (mm)	192
Height (mm)	617
Length (mm)	179
Weight (kg)	34
Connection diameter (mm)	54
Connection type	Threaded

As a result of data validation, we obtain the adjusted value of each of the parameters measured and the value of the refrigerant flow rate (m_{ref}), which has not been measured.

3. Data reduction

The concentrations of the weak and strong solutions were calculated by measuring the density and temperature with two Coriolis flow meters. The properties of the solution were calculated using the correlations reported by Medrano [13].

The absorber load is defined as the heat transfer rate (Q_a) from the solution to the cooling water and calculated from the energy balance at the solution side of the absorber:

$$Q_a = m_{\text{ref}} h_{\text{ref}}\lfloor T_{\text{ref}}, P_a \rfloor + m_w h_w[T_w, x_w] - m_s h_s[T_s, x_s] \tag{4}$$

The refrigerant mass absorbed was determined from the overall mass balance in the absorber:

$$m_{\text{ref}} = m_s - m_w \tag{5}$$

The degree of subcooling of the solution leaving the absorber is defined as the temperature deviation of the actual strong solution from its saturation state at the absorber pressure.

$$\Delta T_{\text{sub}} = T_{\text{eq},s} - T_s \tag{6}$$

The overall heat transfer coefficient was calculated from the absorber load and the logarithmic–mean–temperature–difference as follows.

$$U = \frac{Q_a}{A \Delta T_{\text{LM}}} \tag{7}$$

where

$$\Delta T_{\text{LM}} = \frac{(T_w - T_{\text{cw},o}) - (T_s - T_{\text{cw},i})}{\text{Ln}[(T_w - T_{\text{cw},o})/(T_s - T_{\text{cw},i})]} \tag{8}$$

Table 3
Specifications of the instrumentation used in the experimental set-up

	Instrumentation	Variable measured	Accuracy	Range
1	Coriolis flow meter	Solution flow rate	0.1%	0–1200 $kg \cdot h^{-1}$
		Density	0.5 $kg \cdot m^{-3}$	0–5000 $kg \cdot m^{-3}$
		Temperature	±0.15 °C	0–200 °C
2	Float flow meter	Water flow rate	±2.5%	1200–3000 $kg \cdot h^{-1}$
3	Pressure gauge	Inlet absorber pressure	±0.5%	0–0.5 bar
4	Thermocouple	Temperature	±0.2 °C	−10 to 100 °C

The overall heat transfer coefficient is the inverse of the resultant of three resistances: the convective resistances on the coolant and solution sides, and the conductive resistance of the plate wall. Thus, we have

$$U = \left(\frac{1}{\alpha_{cw}} + \frac{\delta}{k} + \frac{1}{\alpha_s} \right)^{-1} \tag{9}$$

where α_{cw}, the cooling water side heat transfer coefficient, is obtained by applying the following correlation determined experimentally for this plate heat exchanger:

$$\alpha_{cw} = \frac{2b}{k_{cw}} 0.2 Re_{cw}^{0.615} Pr_{cw}^{1/3} \tag{10}$$

By combining Eqs. (4) and (6), the heat transfer coefficient in the absorption side, α_s, is given by the following expression:

$$\alpha_s = \left[\frac{A \Delta T_{LM}}{Q_a} - \frac{\delta}{k} - \frac{1}{\alpha_{cw}} \right]^{-1} \tag{11}$$

The overall mass transfer coefficient can be found from

$$m_{ref} = K A \Delta C_{LM} \tag{12}$$

where the logarithmic mean concentration difference is used for the driving potential:

$$\Delta C_{LM} = \frac{(x_{eq,w}\rho_{eq,w} - x_w \rho_w) - (x_{eq,s}\rho_{eq,s} - x_s \rho_s)}{\mathrm{Ln}[(x_{eq,w}\rho_{eq,w} - x_w \rho_w)/(x_{eq,s}\rho_{eq,s} - x_s \rho_s)]} \tag{13}$$

The absorbed mass flux is defined as the mass flow rate of the refrigerant absorbed per unit of surface area of the plate heat exchanger.

$$j = \frac{m_{ref}}{A} \tag{14}$$

The relative average errors in the estimation of the absorber load, absorbed mass flux, heat transfer coefficient and mass transfer coefficient are around 3%, 3%, 5% and 8%, respectively.

4. Experimental results

Experiments were carried out with both mixtures so that the most suitable spray nozzle could be selected. With this spray nozzle, more experiments were carried out so that the absorption system could be characterised.

4.1. Selection of the spray nozzle

4.1.1. Test with the methanol–TEGDME mixture

To make a preliminary selection, an experiment was carried out for each spray nozzle in the same operation conditions (absorber pressure of 15 kPa, strong solution flow rate of 250 kg·h^{-1}, cooling water temperature of 30 °C and weak solution concentration of 2% by weight).

Fig. 2 shows the parameters that characterise the absorber operation, that is to say the thermal load of the absorber, the degree of subcooling of the strong solution and the overall heat transfer coefficient. It can be seen that the type of spray nozzle significantly affects the operation of the absorber.

The results suggest that the solution needs to be well distributed between the heat exchanger channels. Spray nozzles such as G 1514, which has a small aspersion angle of only 15°, should enable the solution to enter the heat exchanger. This is particularly important because the port diameter of the heat exchanger is relatively small. In order to verify this supposition, experiments were carried out with the two full cone spray nozzles that have the smallest aspersion angles (G 1514 and G 3014 with 15° and 30°, respectively) and a greater solution flow rate.

Table 4 show variations in the strong solution flow rate while the pressure of the absorber is maintained at 15 kPa and the temperature of the cooling water at 30 °C. For all the parameters, except the overall heat transfer coefficient, the spray nozzle G 1514 gave better results. This effect is more pronounced if the solution flow rate is increased.

4.1.2. Test with the TFE–TEGDME mixture

To carry out this study, we selected the spray nozzles that presented the best results for methanol–TEGDME, G 1514, G 3014 and G 6.5, and the spray nozzle HHSJ 6007, which was among the worst. We made this selection to verify if the results followed the trend observed for methanol–TEGDME. Fig. 3 presents the results for these spray nozzles for TFE–TEGDME with a strong solution flow rate of 250 kg·h^{-1}, a weak solution concentration of 25% by weight, an absorber pressure of 5 kPa and a cooling water temperature of 31.5 °C.

Again the spray nozzle HHSJ 6007 gave results far below those for the other three full cone spray nozzles, which were

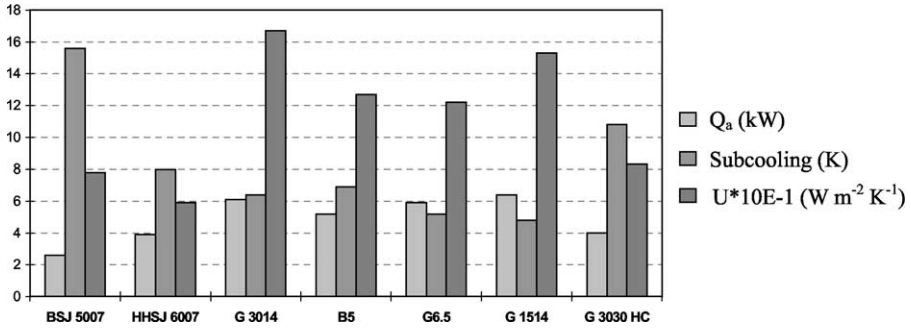

Fig. 2. Comparison of the results obtained with different spray nozzles for the mixture methanol–TEGDME.

Table 4
Comparison of the spray nozzle G 1514 and G 3014 for the mixture methanol–TEGDME

Mixture	Methanol–TEGDME					
Spray nozzle	G 1514			G 3014		
m_s (kg·h^{-1})	250	300	350	250	300	350
Q_a (kW)	6.4	7.0	7.7	6.2	6.3	6.9
Subcooling (K)	4.6	4.8	4.6	5.7	8.0	7.8
U (W·m^{-2}·K^{-1})	153	162	178	157	176	188

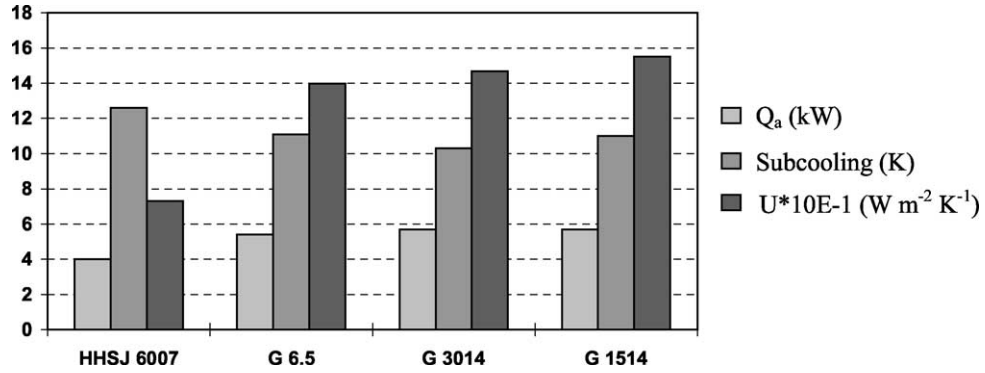

Fig. 3. Comparison of the results obtained with 4 spray nozzles with the mixture TFE–TEGDME.

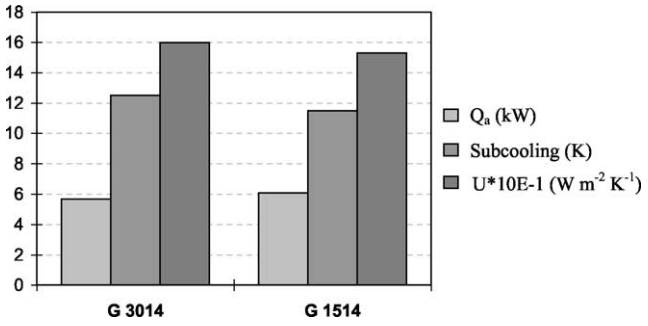

Fig. 4. Comparison of the results obtained with the two narrow angle spray nozzles with the mixture TFE–TEGDME.

very similar. To study the performance at a higher flow rate (350 kg·h^{-1}), experiments were carried out with the two narrow angle spray nozzles. Fig. 4 again confirms that the spray nozzle G 1514 enables slightly higher quantities of vapour to be absorbed, although results of the spray nozzles G 3014 and G 1514 are very similar.

4.1.3. Conclusions for both fluid mixtures

The experiments with the two mixtures indicate that, in both cases, the spray nozzle G 1514 provides the best results of the seven spray nozzles tested in the pilot plant. The difference with respect to other spray nozzles increases as the solution flow rate increases.

This spray nozzle may perform better because the port diameter is small and a spray nozzle with an aspersion angle of only 15 °C is better adapted.

Therefore, this spray nozzle was selected to evaluate the efficiency of the absorption system with the two organic fluid mixtures.

4.2. Characterisation of the absorber operation

After the spray nozzle G 1514 had been selected, the absorption system was characterised. The following parameters were studied: solution flow rate and absorber pressure for different cooling water temperatures.

The effect of the solution mass flow rate on the absorber behaviour was analysed at three cooling water temperatures and at an absorber pressure of 15 kPa for methanol–TEGDME and 5 kPa for TFE–TEGDME. These pressures were identified as being optimum for a thermodynamic analysis of the absorption cycle for air conditioning applications [12]. Furthermore, the influence of the inlet absorber pressure on the absorber performance was investigated in the range 10 to 15 kPa for methanol and 2 to 6 kPa for TFE.

The results will be discussed in terms of the absorber load, absorbed mass flux, degree of subcooling of the strong solution leaving the absorber, solution film heat transfer coefficient and overall mass transfer coefficient.

4.2.1. Effect of the solution mass flow rate

In general terms and for both mixtures, the results show that strong solution temperatures and absorber load increase as the solution mass flow rate increases.

Figs. 5 and 6 show the variation of the absorber load and the degree of subcooling for both mixtures at different cooling water temperatures. The effect of the solution mass flow rate is more pronounced for methanol at a cooling water temperature of 30 °C. In this case, the absorber load varies from 4 to 8 kW for a change in the solution flow rate from 200 to 350 kg·h^{-1}. Moreover, the load for TFE only increases from 5 to 7 kW for the same conditions. This means that in terms of the absorbed mass flux, the values

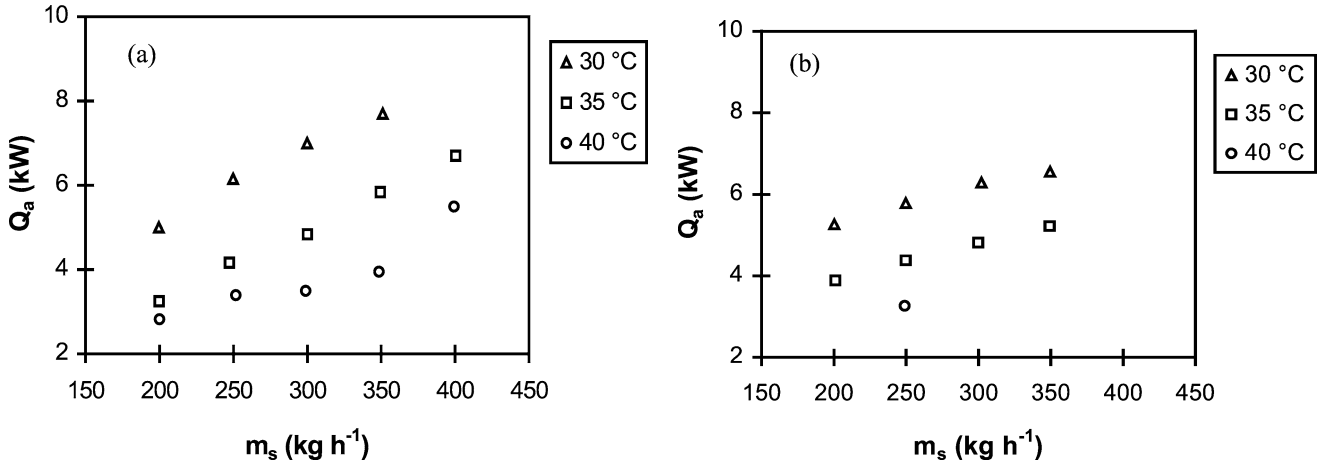

Fig. 5. Effect of the solution mass flow rate on the absorber load: (a) methanol–TEGDME; (b) TFE–TEGDME.

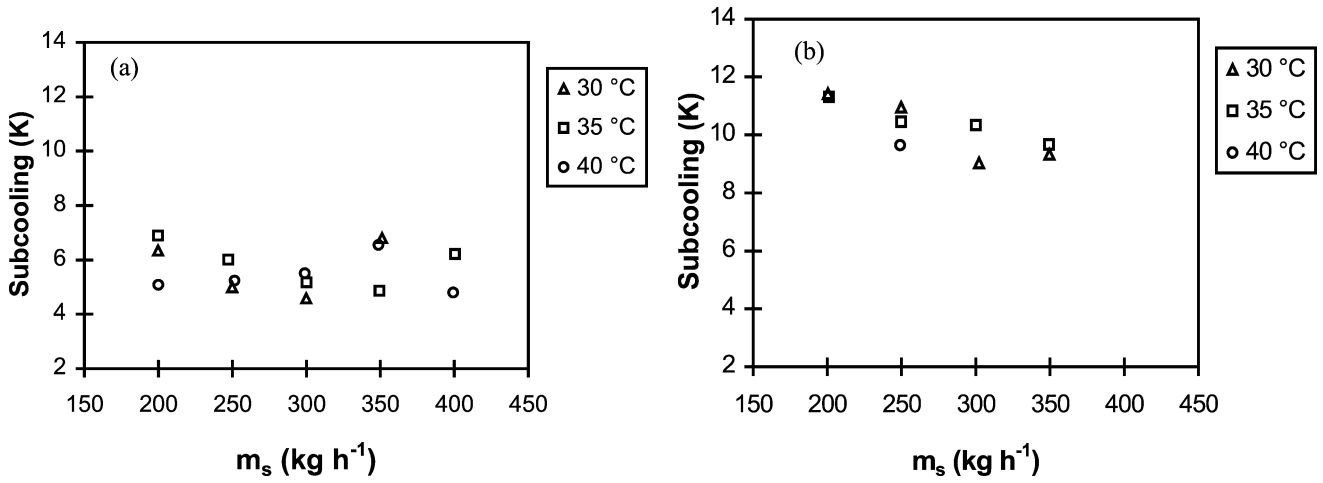

Fig. 6. Effect of the solution mass flow rate on the degree of subcooling at the absorber exit: (a) methanol–TEGDME; (b) TFE–TEGDME.

measured at 30 °C for methanol changed from about 0.4 to 1.2 g·s^{-1}·m^{-2} and for TFE from 1.9 to 2.4 g·s^{-1}·m^{-2}. Both parameters increase as the cooling water temperature decreases for the two mixtures. The absorbed mass flux for TFE–TEGDME is similar to that for the absorption of water–LiBr in vertical falling film tubes [14].

The degree of subcooling and the solution film heat transfer coefficient observed were quite different for both mixtures. The degree of subcooling ranges between 4 and 8 °C for methanol and between 9 and 12 °C for TFE. Increasing the strong solution flow rate causes a drop in the degree of subcooling of the strong solution for TFE (Fig. 6(b)). This is justified by the increase in the strong solution temperature at an almost constant refrigerant concentration. In the case of methanol, the degree of subcooling seems to have a minimum inflection point at around 300 kg·h^{-1} (Fig. 6(a)). The increase in the degree of subcooling at higher solution flow rates may be explained by an increase in the absorber pressure drop. Indeed, for strong solution flow rates over 300 kg·h^{-1}, the absorber pressure drop became significant. At a solution flow rate of 350 kg·h^{-1}, the measured absorber pressure drop was around 0.5 kPa.

The solution film heat transfer coefficient obtained for both mixtures ranges between 100 and 225 W·m^{-2}·K^{-1} and increases slowly with the solution flow rate (Fig. 7). For methanol, the lower the cooling water temperature, the higher the solution film heat transfer coefficient. However, this trend is reversed for TFE. This may be due to the poor transport properties of TFE.

Fig. 8 show the variation of the overall mass transfer coefficient for both mixtures at different cooling water temperatures. Although the transport properties of these organic mixtures are poor compared with those of the inorganic mixtures, the values of the overall mass transfer coefficient obtained in this absorber with the mixture methanol–TEGDME are similar to those obtained in the vertical tube absorber with the mixture water–LiBr [15].

4.2.2. Effect of the absorber pressure

As we have mentioned above, the absorber pressure was set at the optimum value obtained from the thermodynamic simulation of the cycle. However, the compressor provides

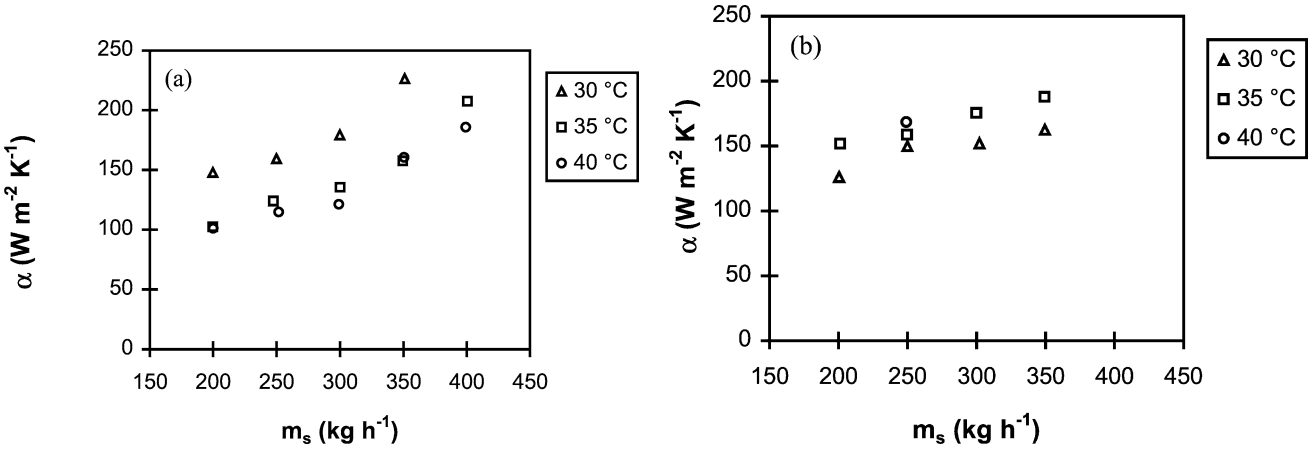

Fig. 7. Effect of the solution mass flow rate on the solution film heat transfer coefficient: (a) methanol–TEGDME; (b) TFE–TEGDME.

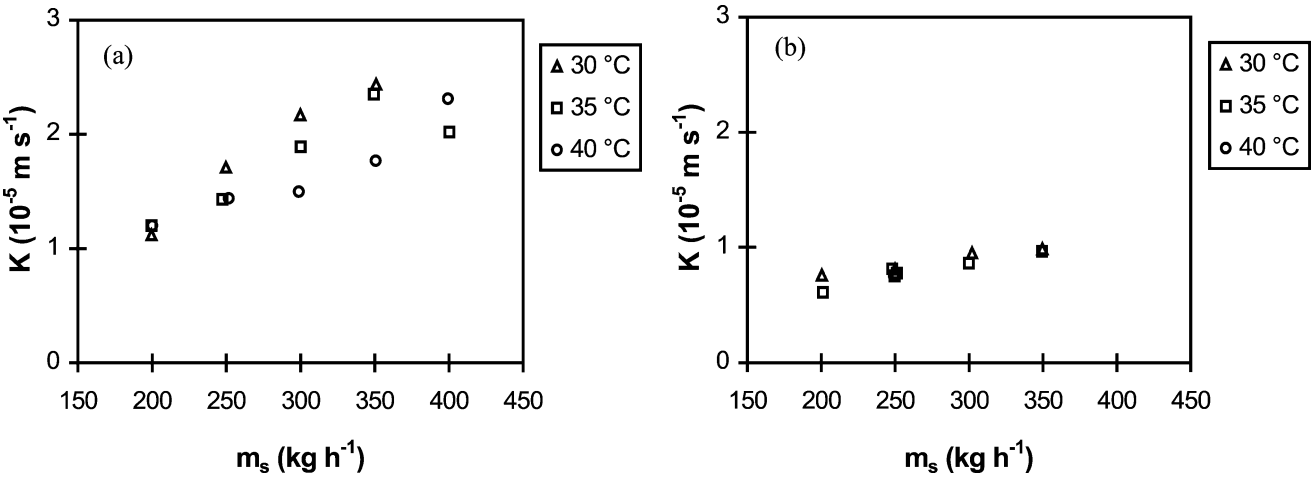

Fig. 8. Effect of the solution mass flow rate on the overall mass transfer coefficient: (a) methanol–TEGDME; (b) TFE–TEGDME.

one degree of freedom more in the cycle, thus increasing the pressure of the absorber with respect to that of the evaporator within the limits permitted by the compressor.

The driving potential for the coupled heat and mass transfer in the absorber depends mainly on the difference between the absorber pressure and the vapour pressure of the refrigerant in the solution. The higher the driving potential, the larger the absorption rate will be.

To study the effect of the operation pressure on the absorber performance, we performed three sets of experiments for methanol at pressures in the range 10–15 kPa. For the refrigerant TFE, we performed experiments in the range 2–6 kPa. Figs. 9–12 show how the pressure affects the absorber operation for both refrigerants. The results were obtained in experiments performed at a cooling water temperature of 30 °C and a solution mass flow rate of 250 kg·h^{-1}.

Fig. 9 shows that increasing the absorber pressure causes a nearly linear increase in the absorber load. The absorber operating with methanol provides about 75% more load when the pressure rises from 10 to 15 kPa. Moreover, when operating with TFE, the additional absorber load is even higher than that for methanol. The absorber load increases from 3 to 7 kW when the inlet pressure increases from 2.5 to 6 kPa.

The effect of the absorber pressure on the degree of subcooling of the strong solution is illustrated in Fig. 10. For methanol, the degree of subcooling decreases as the absorber pressure decreases. Therefore, higher pressures improve the absorber efficiency. In the case of TFE, however, the degree of subcooling is not affected by the pressure and is at a value around 11 °C.

For TFE, the solution film heat transfer coefficient is only slightly affected by the absorber pressure (Fig. 11). Taking into account that the absorber load increases with pressure, this means that the logarithmic-mean temperature difference also increases (from 4 to 11 °C). This reveals that the heat transfer process is clearly unsatisfactory for TFE. However, for methanol, pressure has a greater effect on the solution film heat transfer coefficient, changing it from 100 to 170 W·m^{-2}·K^{-1}, while the logarithmic-mean temperature difference remains constant at about 7 K.

The overall mass transfer coefficient shows a similar trend with the inlet absorber pressure (Fig. 12). The absorber global mass transfer coefficient practically does not vary for

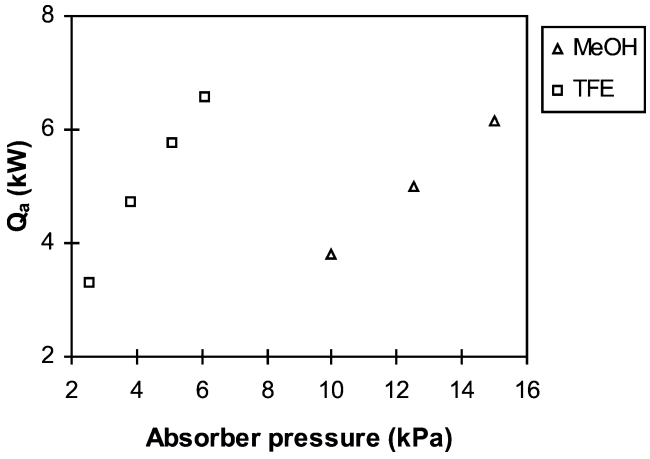

Fig. 9. Effect of the absorber pressure on the absorber load.

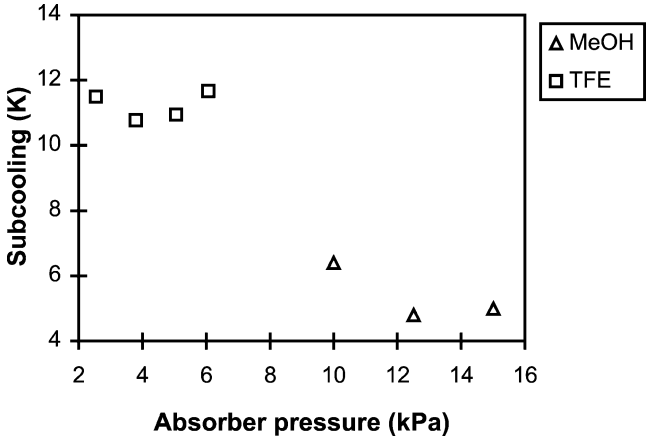

Fig. 10. Effect of the absorber pressure on the degree of subcooling at the absorber exit.

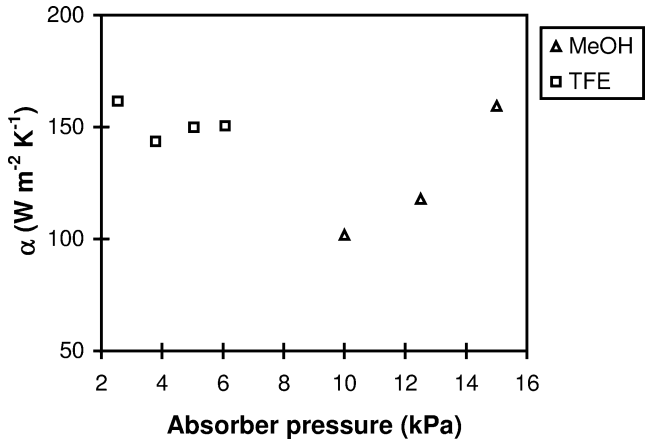

Fig. 11. Effect of the absorber pressure on the solution film heat transfer coefficient.

TFE and remains constant at about 1.0×10^{-5} m·s^{-1}. With the refrigerant methanol shows a higher variation (1.2 to 2.2×10^{-5} m·s^{-1}).

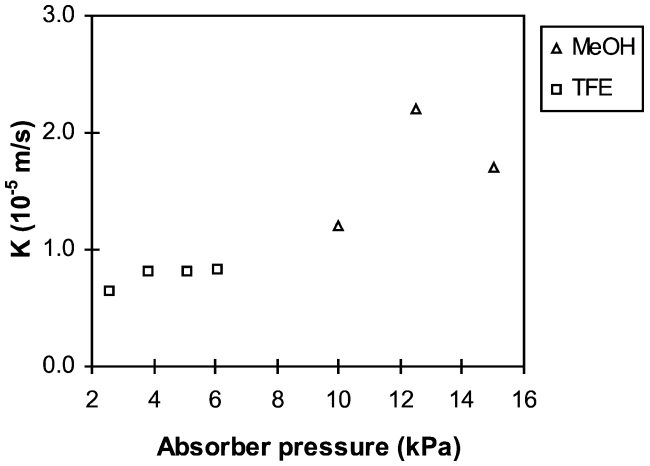

Fig. 12. Effect of the absorber pressure on overall mass transfer coefficient.

5. Conclusions

An absorber test rig for studying the adiabatic absorption process together with the combined absorption–cooling process in a plate heat exchanger was designed and tested in a pilot plant working with organic fluid mixtures.

The performance of the absorber depended heavily on the type of spray nozzle, which should be selected according to the geometry of the absorption system. Despite the poor transport properties of methanol–TEGDME and TFE–TEGDME, the results show that the performance of this kind of absorber with these mixtures is promising.

With methanol–TEGDME, the absorbed mass flux, the solution film heat transfer coefficient and the overall mass transfer coefficient reach values of 0.4 to 1.2 g·s^{-1}·m^{-2}, 100 to 225 W·m^{-2}·K^{-1} and 1.0 to 2.2×10^{-5} m·s^{-1}, respectively. With TFE–TEGDME, the same parameters reach values of 1 to 2.5 g·s^{-1}·m^{-2}, 100 to 170 W·m^{-2}·K^{-1} and 1.0 to 2.2×10^{-5} m·s^{-1}, respectively. Of this is deduced that the results are always better with the mixture methanol–TEGDME. Furthermore, the results obtained with this mixture have improved sensibly increasing the solution flow rate and the absorber pressure.

The principal limitation of this absorption system is the pressure drop in the plate heat exchanger. This limits the cooling load that can be reached with these organic mixtures with a moderately low pressure in the absorber. For strong solution flow rates over 300 kg·h^{-1}, the absorber pressure drop became significant. At a solution flow rate of 350 kg·h^{-1}, the measured absorber pressure drop was around 0.5 kPa. This pressure drop in the plate heat exchanger is less important with those mixtures that have a higher operation pressure in the absorber. For these mixtures it would be possible to use standard plate heat exchangers to build compact machines with a high cooling load.

Acknowledgements

This work was funded by CICYT and FEDER (ClimABgas project 2FD97-0305) in collaboration with Alfa Laval S.A., Clariant Especialidades Químicas and Gas Natural SDG S.A.

References

[1] H. Bokelmann, M. Renz, Thermophysikalische Eigenschaften von Trifluorethanol Stoffsystem für Absorptionswärmepumpen, Ki Klima-Kälte-Heizung 11 (1983) 403–406.
[2] D. Seher, K. Stephan, Trifluoroethanol als Arbeitsstoff für Absorptionswärmepumpen und Absorptionswärmetransformatoren, Ki Klima-Kälte-Heizung 11 (1983) 295–301.
[3] U. Nowaczik, E.L. Schmidt, F. Steimle, New working fluid systems for absorption pumps and absorption heat transformers, in: Proceedings of XVII Internationalen Kältekongresses, Commission B/E, Vienna, Austria, 1987, pp. 815–822.
[4] K. Stephan, R. Hengerer, Heat transformation with the ternary working fluid TFE-H_2O-E181, Internat. J. Refrig. 16 (2) (1993) 120–128.
[5] A. Kawada, M. Otake, M. Toyofuku, Absorption compression heat pump using TFE/E181, in: Proceedings of Absorption Heat Pump Conference, Tokyo, Japan, 1991, pp. 121–125.
[6] M. Ishikawa, H. Kayanuma, N. Issiki, Absorption heat pump using new organic working pairs, in: Proceedings of the International Sorption Heat Pump Conference, Munich, Germany, 1999, pp. 197–204.
[7] M. Narodoslawski, G. Otter, F. Moser, New working pairs for medium and high temperature industrial absorption heat pumps, Heat Recovery Systems 8 (5) (1988) 459–468.
[8] U. Stüven, Entwicklung und Erprobung eines neuen Stoffsystems für den Einsatz in Absorptionswärmetransformatoren, Chem. Ing. Tech. 6 (1989) 486–493.
[9] M. Vallès, D. Boer, A. Coronas, Double effect absorption cycles for air-conditioning using alcohol–polyglycol ethers systems, in: 5th International Energy Agency Conference on Heat Pumping Technologies, Toronto, Canada, 1996, pp. 451–464.
[10] M. Vallès, Experimental study of the absorption process of organic fluids with plate heat exchangers, Ph.D. Thesis, Universitat Rovira i Virgili, Tarragona, Spain, 2000 (in Spanish).
[11] A. Kawada, M. Otake, M. Toyofuku, H. Ota, Absorption heat transformer with TFE/E181, in: Adv. Absorption Workshop, Tokyo, Japan, 1988, pp. 121–126.
[12] D. Boer, M. Vallès, A. Coronas, Performance of double effect absorption compression cycles for air-conditioning using methanol–TEGDME and TFE–TEGDME systems as working pairs, Internat. J. Refrig. 21 (7) (1998) 542–555.
[13] M. Medrano, Development of a modular software package for the simulation of absorption refrigeration and upgrading systems, Research Report TR98-01, Universitat Rovira i Virgili, Tarragona, Spain, 1998 (in Spanish).
[14] B. Tsai, An active enhancement technique for LiBr–H_2O absorbers, Ph.D. Thesis, The Pennsylvania State University, 1997.
[15] W.A. Miller, H. Perz-Blanco, Vertical tube aqueous LiBr falling film absorption using advanced surfaces, in: Proceedings of the International Sorption Heat Pump Conference, AES, Vol. 31, New Orleans, USA, 1994, pp. 185–202.